

Rate Constants of Hydroperoxyl Radical Addition to Cyclic Nitrones: A DFT Study

Frederick A. Villamena,^{*,†,‡} John K. Merle,^{||,⊥} Christopher M. Hadad,^{*,||} and Jay L. Zweier^{*,‡,§}

Department of Pharmacology, Center for Biomedical EPR Spectroscopy and Imaging, The Davis Heart and Lung Research Institute, and Division of Cardiovascular Medicine, Department of Internal Medicine, College of Medicine, and Department of Chemistry, The Ohio State University, Columbus, Ohio 43210

Received: May 11, 2007; In Final Form: July 16, 2007

Nitrones are potential synthetic antioxidants against the reduction of radical-mediated oxidative damage in cells and as analytical reagents for the identification of HO₂[•] and other such transient species. In this work, the PCM/B3LYP/6-31+G(d,p)//B3LYP/6-31G(d) and PCM/mPW1K/6-31+G(d,p) density functional theory (DFT) methods were employed to predict the reactivity of HO₂[•] with various functionalized nitrones as spin traps. The calculated second-order rate constants and free energies of reaction at both levels of theory were in the range of 10⁰–10³ M⁻¹ s⁻¹ and 1 to –12 kcal mol⁻¹, respectively, and the rate constants for some nitrones are on the same order of magnitude as those observed experimentally. The trend in HO₂[•] reactivity to nitrones could not be explained solely on the basis of the relationship of the theoretical positive charge densities on the nitronyl-C, with their respective ionization potentials, electron affinities, rate constants, or free energies of reaction. However, various modes of intramolecular H-bonding interaction were observed at the transition state (TS) structures of HO₂[•] addition to nitrones. The presence of intramolecular H-bonding interactions in the transition states were predicted and may play a significant role toward a facile addition of HO₂[•] to nitrones. In general, HO₂[•] addition to ethoxycarbonyl- and spiro lactam-substituted nitrones, as well as those nitrones without electron-withdrawing substituents, such as 5,5-dimethyl-pyrroline *N*-oxide (DMPO) and 5-spirocyclopentyl-pyrroline *N*-oxide (CPPO), are most preferred compared to the methylcarbamoyl-substituted nitrones. This study suggests that the use of specific spin traps for efficient trapping of HO₂[•] could pave the way toward improved radical detection and antioxidant protection.

I. Introduction

Superoxide radical anion (O₂^{•-}) has attracted considerable attention over the last three decades because it has been shown that O₂^{•-} and O₂^{•-}-derived reactive oxygen species (ROS) such as HO[•], HO₂[•], RO₂[•], RO[•], CO₃^{•-}, and CO₂^{•-} as well as nonradicals such as H₂O₂, HOCl, and ROOH in unregulated concentrations are critical mediators of pathogenesis for various diseases.¹ The formation of hydroperoxyl radical (HO₂[•]) from O₂^{•-} is relevant in both chemical and biological systems. For example, in simple chemical systems, HO₂[•] has been shown to be produced from O₂^{•-} by a proton-transfer reaction from phenol or one-electron reduction of O₂ in the presence of HClO₄.² Furthermore, the presence of a small equilibrium concentration of HO₂[•] in neutral pH (pK_a for HO₂[•] is 4.8³ or 4.4⁴) can contribute to O₂^{•-} instability via a dismutation reaction with a reaction rate of $k = 9.7 \times 10^7 \text{ M}^{-1} \text{ s}^{-1}$.⁵

The generation of HO₂[•] is relevant in the initiation of lipid peroxidation in cellular systems.⁶ In vivo rat heart studies show that the ischemic period (a condition by which the tissues or organs are deprived of blood flow) and immediate reperfusion have enhanced oxygen radical production^{7,8} and are accompa-

nied by ischemia-induced acidosis.⁹ These two processes by which O₂^{•-} can be generated under acidic conditions may have detrimental consequences, resulting in oxidative damage to cellular systems as HO₂[•] is a stronger oxidizer than O₂^{•-} ($E^{\circ} = 1.06$ and 0.94 V , respectively).⁵

Spin trapping¹⁰ with cyclic nitrones in combination with electron paramagnetic resonance (EPR) spectroscopy has been the method of choice for detection of ROS, particularly for O₂^{•-} in biological systems. However, it is not clear if the resulting nitron-O₂H adduct observed by EPR is initially formed from spin trapping of O₂^{•-} or HO₂[•].^{11,12} Therefore, a comparison of the second-order rate constants for the direct addition of HO₂[•] and O₂^{•-} to cyclic nitrones in solution can provide valuable information on the nature of the radical species formed and, hence, be useful in elucidating mechanisms which may involve radical generation in cellular systems.

Nitrones have also been employed as intermediates in the synthesis of natural products¹³ and therapeutic agents.^{14–16} For example, the linear-nitron, disodium-[(*tert*-butylimino)-methyl]-benzene-1,3-disulfonate *N*-oxide (NXY-059) is in clinical trials in the U.S. as a potential therapeutic for neurodegenerative disease.¹⁷ Moreover, the cyclic nitrones, 5,5-dimethyl-pyrroline *N*-oxide (DMPO) and 5-(diethoxyphosphoryl)-5-methyl-1-pyrroline *N*-oxide (DEPMPO) (see Chart 1), have been shown to exhibit cardioprotective properties upon perfusion in a rat's heart after ischemia.¹⁸ However, questions arise regarding the mechanism providing the antioxidant property of nitrones^{15,19} because, for example, DMPO reactivity with O₂^{•-} at physiological pH (~7) is slow, $k = \sim 10 \text{ M}^{-1} \text{ s}^{-1}$, and at pH 5, the rate is on the order of $10^3 \text{ M}^{-1} \text{ s}^{-1}$.²⁰ Therefore, the significantly higher rate

* Corresponding authors. E-mail: Frederick.Villamena@osumc.edu (F.A.V.); hadad.1@osu.edu (C.M.H.); Jay.Zweier@osumc.edu (J.L.Z.). Fax: (614)-688-0999 (F.A.V.); Fax: (614)-292-1685 (C.M.H.); Fax: (614)-247-7799 (J.L.Z.).

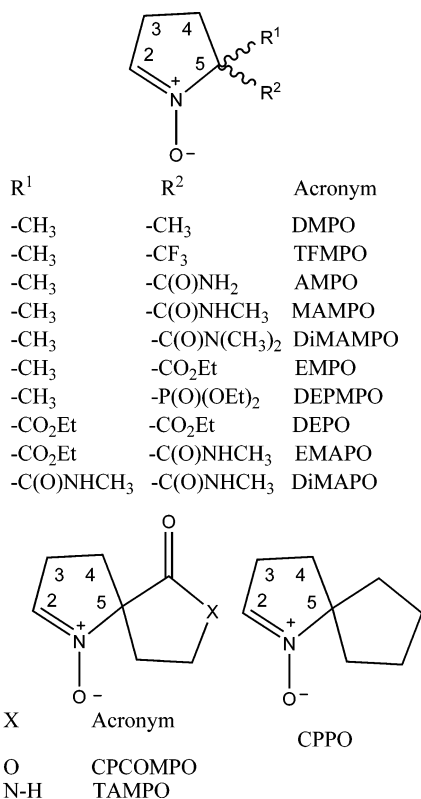
[†] Department of Pharmacology.

[‡] Center for Biomedical EPR Spectroscopy and Imaging.

[§] Division of Cardiovascular Medicine.

^{||} Department of Chemistry.

[⊥] Current address: Department of Chemistry, Winston-Salem State University, Winston-Salem, NC 27110.

CHART 1: DMPO-Type Nitrones Used to Theoretically Investigate Spin Trapping of Hydroperoxyl Radical

of spin trapping of HO₂[•], as compared to O₂^{•-}, with DMPO may partly account for the antioxidant properties of nitrones. However, other mechanisms for the protective property of nitrones against oxidants have also been proposed.^{15,16} Boyd and Boyd²¹ reported the energetics of spin trapping of HO₂[•] by a prototype nitron, H₂C=NHO, with $\Delta E_{\text{MP2}} = -141$ kJ/mol (-33.7 kcal/mol) at the MP2/6-31G(d,p)//HF/6-31G(d) level. Moreover, we previously reported theoretical free energies for O₂^{•-} and HO₂[•] addition to nitrones that have average $\Delta G_{\text{rxn, aq, 298K}} = 10.0 \pm 3.0$ and -7.0 ± 1.6 kcal/mol, respectively.²²

Correctly interpreting the nature of radical species formed in solution is important to accurately elucidate the mechanism(s) for radical production in chemical²³ and biological systems.^{8,24} In a separate study,²⁵ we predicted, and experimentally determined, the bimolecular rate constants for O₂^{•-} addition to various nitron spin traps. However, this work will focus on the prediction of second-order rate constants for HO₂[•] addition to various cyclic nitrones. So far, most of our theoretical work has focused on the prediction of thermodynamic parameters for the spin-trapping of HO₂[•].²² Although thermodynamic data provide insight into the favorability for formation of certain products, they provide no direct information in order to predict the relative rates by which spin trapping occurs. In this study, the second-order rate constants (k_2) in solution for HO₂[•] addition to a variety of important nitrones were theoretically predicted and found to agree well with available experimental values.

II. Computational Methods

General Procedure. Gaussian 03 (revision B.05) was used for all calculations.²⁶ Hybrid density functional theory²⁷ was employed to obtain optimized geometries and vibrational frequencies for all stationary points at the B3LYP/6-31G(d) and mPW1K/6-31+G(d,p) levels.²⁸ The mPW1K calculations were initiated by requesting $\text{iop}(5/45 = 10000428, 5/46 = 05720572, 5/$

TABLE 1: Hydroperoxide Nitron Adduct OOCN Dihedral Angles for the B3LYP/6-31G(d) and mPW1K/6-31+G(d,p) (in Parentheses) Structures

HO ₂ [•] adduct	ϕ (deg)
AMPO- <i>cis</i>	64.7 (66.2)
DEPMPO- <i>trans</i>	76.7 (77.9)
CPCOMPO- <i>cis</i>	56.4 (286.6)
TAMPO- <i>cis</i>	278.2 (270.3)
EMPO- <i>trans</i>	76.4 (77.3)
TFMPO- <i>trans</i>	77.3 (78.9)
CPPO	75.7 (76.7)
DMPO	75.9 (76.9)
DEPO	62.6 (62.3)
MAMPO- <i>cis</i>	64.4 (66.1)
DiMAMPO- <i>cis</i>	77.6 (79.4)
DiMAPO	78.4 (78.4)
EMAPO- <i>cis</i> ^a	64.2 (65.7)
EMAPO- <i>trans</i> ^a	62.2 (40.3)
MSMPO- <i>trans</i>	78.1 (79.4)

^a Where the -OOH groups are *cis* or *trans* to the amide group.

47 = 10001000) in the route card. The mPW1K method has been shown by Truhlar and co-workers to be very effective for determining transition state (TS) structures and barrier heights for H-atom transfer reactions.²⁹ Single-point energies on the optimized B3LYP/6-31G(d) geometries were obtained at the B3LYP/6-31+G(d,p) level. The effect of solvation was investigated via single-point energy calculations at the B3LYP/6-31+G(d,p) level using the polarizable continuum model (PCM) to represent water.³⁰ Stationary points, as minima for both the nitron spin traps and their respective HO₂[•] adducts, were determined to have zero imaginary vibrational frequencies as derived from a harmonic vibrational frequency analysis at the level at which the stationary points were optimized. Scaling factors of 0.9806³¹ and 0.9515³² were used for zero-point vibrational energy (ZPE) corrections for the B3LYP and mPW1K geometries, respectively. Free energies were obtained from the calculated thermal and entropic corrections at 298 K using the unscaled vibrational frequencies. For the minima, spin contamination values for the radical adducts are negligible, i.e., $0.75 < \langle S^2 \rangle < 0.80$ (see Tables S2–S7, Supporting Information). Spin densities (populations) and charge densities were obtained from a natural population analysis (NPA) of the electronic wavefunctions at the PCM/B3LYP/6-31+G(d,p)//B3LYP/6-31G(d) and PCM/mPW1K/6-31+G(d,p) levels.³³

Initial nitron and spin-adduct structures for transition state (TS) searches were chosen based on the most stable conformer/configuration resulting from the PCM aqueous phase energies. Transition states (TS) were confirmed to have one imaginary vibrational frequency and, furthermore, shown to be connected to the desired reactant and product by displacement along the normal coordinate (typically 10%) for the imaginary vibrational frequency in the positive and negative directions followed by careful minimization using $\text{opt} = \text{calcfc}$. Hence, all HO₂[•] adduct structures reported here are the result of minimizing the energy of the displaced TS structures.

To predict rate constants, we examined the potential energy surfaces and located maxima, and we have been successful in locating a variety of TS's for such reactions in the recent past.^{22,25,34} The $\langle S^2 \rangle$ values for the TS have typically shown

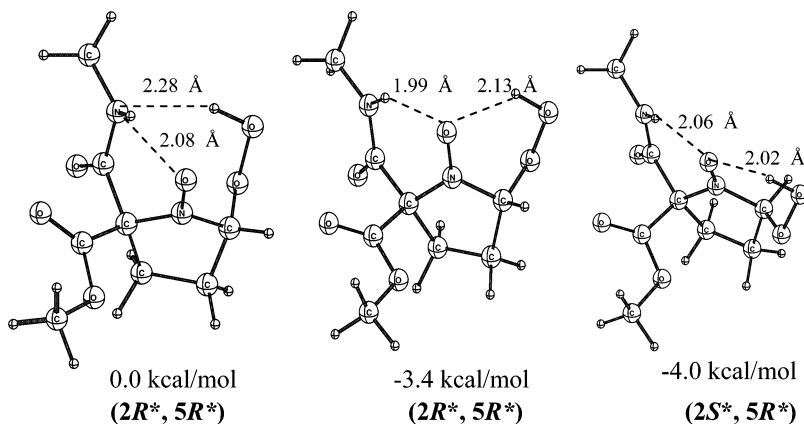


Figure 1. Relative free energies in aqueous solution ($G_{298\text{K,aq}}$ in kcal/mol) of various optimized EMAPO HO_2^* adducts showing strong intramolecular interactions at the PCM/B3LYP/6-31+G(d,p)/B3LYP/6-31G(d) level. Note that the preferred isomer is $(2S^*,5R^*)$ -EMAPO- O_2H in which the hydroperoxyl moiety is *trans* to the amide group.

minimal spin contamination, i.e., $0.81 < \langle S^2 \rangle < 0.82$. Conventional transition state theory (TST) was utilized to estimate the rates for spin-adduct formation at 298 K.³⁵ The conventional TST rate equation in the thermodynamic formulation as a function of temperature is as follows:

$$k(T)_{\text{TST}} = \Gamma(T) \frac{k_{\text{B}}T}{h} \exp(-\Delta G_0^\ddagger/k_{\text{B}}T) \quad (1)$$

In eq 1, T is the absolute temperature, h is Planck's constant, k_{B} is Boltzmann constant, and ΔG_0^\ddagger is the free energy barrier height relative to reactants at infinite separation. The temperature-dependent factor $\Gamma(T)$ represents quantum mechanical tunneling and is accounted for by the Wigner approximation:³⁶

$$\Gamma(T) = 1 + \left(\frac{1}{24}\right) \left[1.44 \frac{\nu_i}{T}\right]^2 \quad (2)$$

in which ν_i is the imaginary vibrational frequency representing the TS barrier's curvature.

III. Results and Discussion

A. Nitrones and Hydroperoxyl Adducts. Selected bond distances for the B3LYP/6-31G(d) optimized geometries of the nitrone spin traps and their corresponding HO_2^* adducts are shown in Table S1 of the Supporting Information. All of the relevant bond distances for the nitrone and nitroxyl moieties as well as the various electron-withdrawing substituents are in good agreement with reported experimental X-ray crystallographic bond lengths for related compounds.³⁷

We previously²⁵ established, by a computational approach, that in aqueous solution, the amide functionality of AMPO, MAMPO, and DiMAPO (Chart 1) are predominantly in the amide form (or lactam form for TAMPO) rather than in the respective imidic acid (or lactim) form. Spin-adduct structures have O–O bond distances from 1.41 to 1.42 Å in all of the HO_2^* adducts. The $\text{C}_{\text{ring}}\text{--O}_2\text{H}$ bond distances are in the 1.37–1.43 Å range, similar to that observed experimentally for cyclic hydroperoxides (~ 1.46 Å).³⁸ The conformations for various HO_2^* adducts with nitrones obtained at the B3LYP/6-31G(d) level correlate well with those at the mPW1K/6-31+G(d,p) level of theory (Table 1), with the exception of CPCOMPO- O_2H in which the predicted O–O–C–N dihedral angle is smaller (56.4°) at the B3LYP/6-31G(d) level as compared to mPW1K/6-31+G(d,p) (286.6°). An $\text{O}_2\text{H}\text{---O}\text{---N}$ H-bonding interaction was observed for the HO_2^* adducts of DiMAMPO, DiMAPO, DEPMPO, DMPO, TFMPO, MSMPO, CPPPO, and EMPO, with

an H---O bond distance ranging from 2.04 to 3.09 Å. An $\text{O}_2\text{H}\text{---O}=\text{C}$ H-bonding interaction was predicted for DEPO, CP-COMPO, and TAMPO with H---O distances between 1.84 and 1.99 Å, while an $\text{O}_2\text{H}\text{---NR}_2$ interaction was predicted for AMPO, MAMPO, and EMAPO with H---N distances of 2.30 to 2.42 Å. (See Figure S1 of the Supporting Information for the mPW1K/6-31+G(d,p) structural parameters.)

Figure 1 shows the most favored diastereomer $(2S,5R)$ for the EMAPO- O_2H adduct in which the amide group is *trans* to the HO_2 moiety. The preferred $(2S,5R)$ isomer for EMAPO- O_2H exhibits two intramolecular H-bond interactions, (i.e., N–O---H–N and OOH---O–N), which are *trans* to each other and are more stable than the $(2R,5R)$ isomer by -0.6 kcal/mol.

B. Transition State Structures. The TS structures for HO_2^* addition to the nitrones were calculated, and each stationary point gave a single imaginary vibrational frequency corresponding to motion along the $\text{C}_2\text{--O}_2\text{H}$ bond axis (Table 2). The TSs for HO_2^* addition have imaginary vibrational frequencies ranging from $323i$ to $517i$ cm^{-1} at the B3LYP/6-31G(d) level and $312i$ to $411i$ cm^{-1} at the mPW1K/6-31+G(d,p) level (Table 2).

The transition states have a narrow range of $\text{C}_2\text{---O}_2\text{H}$ distances, ranging from 2.00 to 2.12 Å and 2.10 to 2.15 Å at the B3LYP/6-31G(d) and mPW1K/6-31+G(d,p) levels, respectively. These calculated $\text{C}_2\text{---O}_2\text{H}$ distances are intermediate between the distances calculated for the complexed form and the final adduct as a product (Table 2). The TS structures for HO_2^* addition have average sums of the bond angles around the C_2 carbon of $356.6 \pm 1.0^\circ$, intermediate to those predicted for the nitrones ($360.0 \pm 0.1^\circ$) and their respective HO_2^* adduct products ($328.1 \pm 1.2^\circ$). In light of Hammond's postulate, the sums of the bond angles suggest that the TS for HO_2^* addition is early on the reaction coordinate; i.e., the TS structures are closer to the reactants.

Table 3 shows the spin density distribution for the various TS structures for HO_2^* addition at the B3LYP/6-31+G(d,p)//B3LYP/6-31G(d), and they are all very similar. The average spin densities (populations) on the nitronyl-N, nitronyl-O, hydroperoxyl- β -O, and hydroperoxyl- γ -O atoms are 0.18 ± 0.03 , 0.30 ± 0.03 , 0.52 ± 0.03 , and 0.17 ± 0.02 e, respectively. The same trend has been observed at the mPW1K/6-31+G(d,p) level (Table S8, Supporting Information). The calculated spin densities for the HO_2^* atoms are 0.73 e for the distal O and 0.27 e on the proximal O relative to H, indicating that some electron transfer occurs from the HO_2^* to the nitrone in the TS. We note that this behavior is contrary to the reaction of hydroxyl radical with electron-rich aromatic rings for which

TABLE 2: Relative Enthalpies, $\Delta H_{298\text{K}}$, and Free Energies, $\Delta G_{298\text{K}}$ (kcal/mol), in Aqueous Solution and Other Structural Parameters for the Transition State Structures for HO_2^* Addition at the PCM/mPW1K/6-31+G(d,p)//mPW1K/6-31+G(d,p) and PCM/B3LYP/6-31+G(d,p)//B3LYP/6-31G(d) (in Parentheses) Levels of Theory

structure	$\Delta H_{298\text{K, aq}}^e$	$\Delta G_{298\text{K, aq}}^e$	C--- O_2H Å	$\langle S^2 \rangle^f$	imaginary frequency ^g
AMPO					
AMPO + O_2H^a	0.0 (0.0)	0.0 (0.0)	∞	<i>a</i>	
AMPO--- O_2H^b	2.6 (2.8)	12.3 (13.0)	3.29 (3.24)	0.75 (0.75)	0
[AMPO--- $\text{O}_2\text{H}]^{\ddagger c}$	5.3 (5.1)	17.5 (17.5)	2.10 (2.10)	0.81 (0.80)	359 <i>i</i> (354 <i>i</i>)
AMPO- O_2H^d	-18.0 (-14.6)	-5.5 (-1.6)	1.42 (1.40)	0.75 (0.75)	0
DEPMPO					
DEPMPO + O_2H	0.0 (0.0)	0.0 (0.0)	∞	<i>a</i>	
DEPMPO--- O_2H	(-3.1)	(6.7)	3.20 (3.55)	0.75 (0.75)	0
[DEPMPO--- $\text{O}_2\text{H}]^{\ddagger}$	4.5 (5.1)	16.6 (17.3)	2.12 (2.10)	0.81 (0.79)	383 <i>i</i> (416 <i>i</i>)
DEPMPO- O_2H	-21.0 (-17.5)	-8.6 (-4.8)	1.41 (1.41)	0.75 (0.75)	0
DMPO					
DMPO + O_2H	0.0 (0.0)	0.0 (0.0)	∞	<i>a</i>	
DMPO--- O_2H	-4.5 (-3.6)	4.8 (6.0)	3.68 (3.01)	0.75 (0.75)	0
[DMPO--- $\text{O}_2\text{H}]^{\ddagger}$	4.3 (4.7)	15.8 (16.5)	2.12 (2.10)	0.81 (0.79)	380 <i>i</i> (415 <i>i</i>)
DMPO- O_2H	-20.1 (-16.7)	-8.2 (-4.6)	1.41 (1.42)	0.76 (0.75)	0
EMPO					
EMPO + O_2H	0.0 (0.0)	0.0 (0.0)	∞	<i>a</i>	
EMPO--- O_2H	-4.4 (-3.8)	4.4 (5.6)	3.56 (3.48)	0.75 (0.75)	0
[EMPO--- $\text{O}_2\text{H}]^{\ddagger}$	4.1 (4.5)	15.1 (15.9)	2.13 (2.10)	0.81 (0.80)	364 <i>i</i> (413 <i>i</i>)
EMPO- O_2H	-20.7 (-17.5)	-9.5 (-6.2)	1.41 (1.42)	0.76 (0.75)	0
CPCOMPO					
CPCOMPO + O_2H	0.0 (0.0)	0.0 (0.0)	∞	<i>a</i>	
CPCOMPO--- O_2H	1.0 (1.2)	9.8 (10.5)	3.60 (3.67)	0.75 (0.75)	0
[CPCOMPO--- $\text{O}_2\text{H}]^{\ddagger}$	4.8 (4.8)	17.0 (17.3)	2.11 (2.10)	0.83 (0.80)	387 <i>i</i> (323 <i>i</i>)
CPCOMPO- O_2H	-21.7 (-17.7)	-8.7 (-4.7)	1.41 (1.42)	0.75 (0.75)	0
TAMPO					
TAMPO + O_2H	0.0 (0.0)	0.0 (0.0)	∞	<i>a</i>	
TAMPO--- O_2H	-1.5 (-1.1)	7.5 (8.6)	4.50 (4.60)	0.75 (0.75)	0
[TAMPO--- $\text{O}_2\text{H}]^{\ddagger}$	2.6 (2.4)	15.0 (15.0)	2.10 (2.12)	0.83 (0.81)	391 <i>i</i> (365 <i>i</i>)
TAMPO- O_2H	-21.6 (-18.2)	-8.5 (-4.9)	1.41 (1.42)	0.75 (0.75)	0
MSMPO					
MSMPO + O_2H	0.0 (0.0)	0.0 (0.0)	∞	<i>a</i>	
MSMPO--- O_2H	-3.5 (-2.7)	6.5 (7.2)	3.64 (3.51)	0.75 (0.75)	0
[MSMPO--- $\text{O}_2\text{H}]^{\ddagger}$	4.8 (5.0)	16.7 (16.9)	2.14 (2.10)	0.81 (0.80)	387 <i>i</i> (439 <i>i</i>)
MSMPO- O_2H	-22.6 (-19.4)	-10.2 (-7.3)	1.41 (1.41)	0.75 (0.75)	0
TFMPO					
TFMPO + O_2H	0.0 (0.0)	0.0 (0.0)	∞	<i>a</i>	
TFMPO--- O_2H	-3.6 (-2.7)	5.9 (7.2)	3.60 (3.49)	0.75 (0.75)	0
[TFMPO--- $\text{O}_2\text{H}]^{\ddagger}$	4.6 (5.3)	16.1 (17.2)	2.13 (2.11)	0.81 (0.80)	380 <i>i</i> (412 <i>i</i>)
TFMPO- O_2H	-21.3 (-17.8)	-9.4 (-5.8)	1.41 (1.41)	0.75 (0.75)	0

^a At infinite separation. ^b Nitron- HO_2^* complex. ^c Transition state. ^d Products. ^e Values are relative energies based on single-point energy calculations with the polarizable continuum model (PCM) at the mPW1K/6-31+G(d,p) level using water as a solvent. Values in parentheses are at the PCM/B3LYP/6-31+G(d,p)//B3LYP/6-31G(d) level. Thermal and entropic corrections from the gas-phase calculations were applied with the single-point energy for the PCM level in order to get an estimated $\Delta H_{298\text{K}}$ and $\Delta G_{298\text{K}}$ in water. ^f The $\langle S^2 \rangle$ for all the nitrones is 0.00 while that of HO_2^* is 0.75 at both levels of theory used. ^g Point group for all structures is C_1 and imaginary vibrational frequencies are in the units of cm^{-1} .

electron density from the aromatic unit is transferred to the hydroxyl moiety.³⁹ The final HO_2^* adduct structures show almost complete spin-population transfer to the nitroxyl moiety with spin densities of 0.43 and 0.52 e on the nitroxyl N and O, respectively.

The OOH---O=C , OOH---NR_2 , and OOH---O-N H-bond distances in the transition states are very similar to H-bond distances observed in their respective product structures with deviations of 0.1–0.3 Å (Figure S1, Supporting Information). These predicted interactions play a significant role in stabilizing the TS structures and, hence, in the facile formation of the adducts as products. All predicted TS H-bonding interactions are present for both B3LYP/6-31G(d) and mPW1K/6-31+G(d,p) optimized structures.

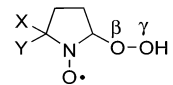
C. Calculated Bimolecular Rate Constants. In our previous studies,^{11,40} we showed that the direct addition of HO_2^* to DMPO is one of the two possible mechanisms for the formation of $\text{DMPO-O}_2\text{H}$ in aqueous solution with $\text{O}_2^{\bullet-}$ addition followed by proton transfer being the other. This reaction is relevant

because the generation of $\text{O}_2^{\bullet-}$ in acidic conditions can favor direct radical addition of HO_2^* instead of $\text{O}_2^{\bullet-}$ to DMPO. The free energies for $\text{O}_2^{\bullet-}$ protonation by hydronium ion in an aqueous medium is highly exoergic: $\Delta G_{\text{rxn}-1, \text{aq}} = -41.1$ and -40.5 kcal/mol at the PCM/mPW1K/6-31+G(d,p) and PCM/B3LYP/6-31+G(d,p)//B3LYP/6-31G(d) levels, respectively (see Table 4).

Reactions for HO_2^* addition to nitrones are exoergic, with $\Delta G_{\text{rxn}-2, \text{aq}}$ (Table 4) values that range from -5.1 to -11.5 kcal/mol, while $\text{O}_2^{\bullet-}$ additions to nitrones are endoergic, with $\Delta G_{\text{aq}} = 0.7$ – 8.3 kcal/mol at the PCM/mPW1K/6-31+G(d,p) level.²⁵ These free energies of reaction are consistent with the experimental reduction potentials of $E^\circ = 1.06$ and 0.94 V for HO_2^* and $\text{O}_2^{\bullet-}$, respectively.⁴¹ The free energies of reaction for HO_2^* reactions with nitrones follow the order of increasing (more positive) ΔG_{rxn} (in kcal/mol): MSMPO (-10.2) > DEPO (-10.1) > EMPO (-9.5) > TFMPO (-9.4) > DiMAMPO (-8.9) > CPCOMPO (-8.7) > DEPMPO (-8.6) > TAMPO (-8.5) > DMPO (-8.2) > EMAPO trans addition to

TABLE 3: NPA Charges and Spin Densities (Populations) of Transition States for the Formation of Various Hydroperoxyl Adducts at the B3LYP/6-31+G(d,p)//B3LYP/6-31G(d) Level in Units of Electrons

NPA Charges and Spin Densities (α - β)



	N	O _{nitroxy}	β -O	γ -O
AMPO	0.02, 0.17	-0.50, 0.28	-0.26, 0.53	-0.41, 0.18
DEPMPO	0.02, 0.19	-0.51, 0.27	-0.26, 0.53	-0.42, 0.16
DMPO	0.04, 0.18	-0.50, 0.28	-0.27, 0.53	-0.43, 0.15
EMPO	0.04, 0.18	-0.49, 0.29	-0.27, 0.53	-0.43, 0.16
CPCOMPO	0.04, 0.16	-0.47, 0.29	-0.28, 0.54	-0.40, 0.19
TAMPO	0.04, 0.18	-0.47, 0.31	-0.25, 0.53	-0.43, 0.17
MSMPO	0.01, 0.18	-0.47, 0.31	-0.27, 0.52	-0.42, 0.16
TFMPO	0.03, 0.17	-0.48, 0.29	-0.26, 0.54	-0.42, 0.17
DEPO	0.03, 0.15	-0.44, 0.33	-0.28, 0.51	-0.41, 0.19
CPPO	0.04, 0.19	-0.51, 0.27	-0.26, 0.53	-0.43, 0.16
MSMPO	0.01, 0.18	-0.47, 0.31	-0.27, 0.52	-0.42, 0.16
MAMPO	0.01, 0.22	-0.46, 0.37	-0.29, 0.44	-0.44, 0.13
DiMAMPO	0.03, 0.19	-0.51, 0.26	-0.25, 0.55	-0.43, 0.16
DiMAPO	0.03, 0.26	-0.47, 0.36	-0.28, 0.43	-0.44, 0.11
EMAPO-cis	0.03, 0.16	-0.49, 0.28	-0.26, 0.53	-0.40, 0.19
EMAPO-trans	0.02, 0.17	-0.49, 0.28	-0.26, 0.53	-0.40, 0.20

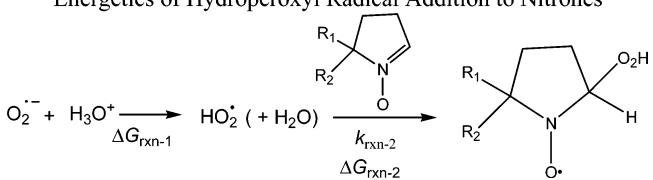
amide group (-8.0) > DiMAPO (-5.6) > AMPO (-5.5) > MAMPO = EMAPO cis addition to amide group (5.1) and the *N*-monoalkylamide substituted nitrones MAMPO, DiMAPO, and EMAPO (Table 4). In contrast to the predicted thermodynamics for the O₂^{•-} additions to amide-substituted nitrones which is the most favorable, the HO₂[•] additions to *N*-monoalkylamide substituted nitrones were not the most thermodynamically favored.²⁵

At the PCM/mPW1K/6-31+G(d,p)//mPW1K/6-31+G(d,p) level, the calculated rate constants, $k_{\text{rxn}-2}$, for HO₂[•] addition to nitrones are the greatest for DEPO ($k_{\text{rxn}-2} = 3.0 \times 10^3 \text{ M}^{-1} \text{ s}^{-1}$) followed by TAMPO ($k_{\text{rxn}-2} = 1.9 \times 10^3 \text{ M}^{-1} \text{ s}^{-1}$), trans addition to the amide moiety of EMAPO ($k_{\text{rxn}-2} = 1.4 \times 10^3 \text{ M}^{-1} \text{ s}^{-1}$), EMPO ($k_{\text{rxn}-2} = 1.5 \times 10^3 \text{ M}^{-1} \text{ s}^{-1}$), CPPO ($k_{\text{rxn}-2} = 1.1 \times 10^3 \text{ M}^{-1} \text{ s}^{-1}$), and DMPO ($k_{\text{rxn}-2} = 1.0 \times 10^3 \text{ M}^{-1} \text{ s}^{-1}$). The TFMPO, DEPMPO, and MSMPO nitrones have intermediate rate constants with values $k_{\text{rxn}-2} = 276.0, 125.8,$ and $105.9 \text{ M}^{-1} \text{ s}^{-1}$, respectively. The nitrones that have the smallest rate constants for HO₂[•] addition are the amide-nitrones, i.e., AMPO, MAMPO, DiMAMPO, DiMAPO, and EMAPO (where the HO₂[•] addition is cis to the amide group), as well as CPCOMPO where the rate constants are in the range 1.3–61.9 M⁻¹ s⁻¹ (see Table 4). The same qualitative trend is predicted at the PCM/B3LYP/6-31+G(d,p)//B3LYP/6-31G(d) level, with the exception of DEPMPO.

The electronic and thermodynamic parameters including the C₂ charge densities, rate constants, free energies, electron affinities, and ionization potentials calculated at the PCM/mPW1K/6-31+G(d,p)//mPW1K/6-31+G(d,p) level correlate well with those calculated at the PCM/B3LYP/6-31+G(d,p)//B3LYP/6-31G(d) level of theory as shown in the Figure S2 of the Supporting Information. However, the preference for HO₂[•] addition to certain nitrones does not follow the same trend observed for O₂^{•-} addition that we reported recently²⁵ in which we demonstrated a dependence of $k_{\text{rxn}-2}$ and $\Delta G_{\text{rxn}-2}$ on the C₂ charge density of the nitronone. The PCM/mPW1K/6-31+G(d,p)//mPW1K/6-31+G(d,p) $k_{\text{rxn}-2}$ and $\Delta G_{\text{rxn}-2}$ values for HO₂[•] addition to nitrones give a poor correlation with nitronone C₂ charge densities (see Figure S3a,b, Supporting Information). Poor correlation also resulted from the PCM/B3LYP/6-31+G-

TABLE 4: Aqueous Phase Charge Densities of the Nitronyl-C (C₂), Electron Affinities, Ionization Potentials (eV) of the Nitrones, Rate Constants (k , M⁻¹, s⁻¹), and Free Energies of Reaction^a (ΔG_{rxn} , kcal/mol) for the Formation of Hydroperoxyl Adducts at the PCM/mPW1K/6-31+G(d,p) and PCM/B3LYP/6-31+G(d,p)//B3LYP/6-31G(d) Levels of Theory

Energetics of Hydroperoxyl Radical Addition to Nitrones



entry	PCM/mPW1K/6-31+G(d,p)//mPW1K/6-31+G(d,p)					PCM/B3LYP/6-31+G(d,p)//B3LYP/6-31G(d)				
	C ₂ Charge (e)	EA ^{d,f} (eV)	IP ^{e,f} (eV)	$k_{\text{rxn}-2}$	$\Delta G_{\text{rxn}-2}$	C ₂ Charge (e)	EA ^{d,f} (eV)	IP ^{e,f} (eV)	$k_{\text{rxn}-2}$	$\Delta G_{\text{rxn}-2}$
AMPO	0.054	-1.90 (0.10) ^f	6.27 (8.22) ^f	26.6	-5.5	0.060	-1.91 (0.68)	6.33 (8.01)	25.0	-1.6
DEPMPO	0.038	-1.74 (0.32)	6.22 (7.78)	125.8	-8.6	0.043	-1.63 (0.61)	6.26 (7.59)	71.7	-4.8
CPCOMPO	0.04	-1.92 (0.15)	6.33 (8.27)	61.9	-8.7	0.045	-2.32 (0.04)	6.37 (8.06)	39.2	-4.7
TAMPO	0.034	-1.69 (0.39)	6.18 (7.98)	1936.5	-8.5	0.038	-1.64 (1.11)	6.21 (7.75)	1835.0	-4.9
EMPO	0.035	-1.73 (0.37)	6.22 (8.02)	1528.4	-9.5	0.040	-1.77 (0.86)	6.25 (7.81)	411.9	-6.2
TFMPO	0.038	-1.88 (0.29)	6.33 (8.36)	276.0	-9.4	0.043	-1.91 (0.96)	6.39 (8.13)	48.3	-5.8
CPPO	0.015	-1.55 (0.73)	6.04 (7.94)	1140.6	-8.5	0.024	-1.63 (1.29)	6.04 (7.72)	294.2	-4.8
DMPO	0.013	-1.54 (0.73)	6.06 (7.98)	1002.3	-8.2	0.019	-1.56 (1.38)	6.09 (7.79)	285.5	-4.6
DEPO	0.039	-1.85 (0.25)	6.33 (7.96)	2982.3	-10.1	0.043	-2.87 (-0.81)	6.36 (7.71)	2073.0	-6.2
MSMPO	0.047	-3.14 (-1.47)	6.34 (8.08)	105.9	-10.2	0.053	-3.44 (-0.86)	6.37 (7.88)	73.5	-7.3
MAMPO	0.056	-1.92 (0.12)	5.74 (7.65)	4.6	-5.1	0.060	-1.93 (0.68)	5.95 (7.58)	17.7	-0.7
DiMAMPO	0.026	-0.67 (0.73)	6.08 (7.64)	1.3	-8.9	0.030	-1.53 (0.72)	6.08 (7.35)	0.6	-4.7
DiMAPO	0.092	-2.20 (-0.38)	6.037 (8.15)	5.8	-5.6	0.098	-2.21 (0.11)	6.36 (7.87)	32.6	-2.9
EMAPO (cis) ^b	0.069	-2.08 (-0.08)	5.89 (7.47)	3.0	-5.1	0.073	-2.10 (0.46)	6.08 (7.38)	1.5	-0.9
EMAPO (trans) ^c	0.069	n/a	n/a	1359.0	-8.0	0.073	n/a	n/a	876.2	-4.5
HOO* ^g	n/a	-4.02 (-0.80) ^g	8.33 (11.98)	n/a	n/a	n/a	-4.22 (0.29)	8.47 (11.88)	n/a	n/a

^a $\Delta G_{\text{rxn}-1} = -41.1$ kcal/mol at the PCM/mPW1K/6-31+G(d,p)//mPW1K/6-31+G(d,p) or -40.5 kcal/mol at the PCM/B3LYP/6-31+G(d,p)//B3LYP/6-31G(d). Energetics are derived from the hydroperoxyl radical adduct structures resulting from the 10% displacement of their respective TS structure. ^b Adduct has the hydroperoxyl moiety cis to the amide group. ^c Adduct has the hydroperoxyl moiety trans to the amide group (or cis to the ester group). ^d Calculated as EA = $\Delta H_{298\text{K}}$ (radical anion) - $\Delta H_{298\text{K}}$ (neutral) ^e Calculated as IP = $\Delta H_{298\text{K}}$ (radical cation) - $\Delta H_{298\text{K}}$ (neutral). ^f Values in parentheses are in gas phase. ^g Calculated EA and IP for HO₂[•] are defined as EA = $\Delta H_{298\text{K}}$ (HO₂⁻) - $\Delta H_{298\text{K}}$ (HO₂[•]) and IP = $\Delta H_{298\text{K}}$ (HO₂⁺) - $\Delta H_{298\text{K}}$ (HO₂[•]). The absolute EA for HO₂[•] in the gas phase is 0.80 eV at the mPW1K/6-31+G(d,p) level (EA_{exptl} = 1.089 ± 0.006 eV).⁴⁴

(d,p)//B3LYP/6-31G(d) values (see Figure S4a,b, Supporting Information). The poor correlation between the C₂ charge densities and the favorability of HO₂[•] addition to nitrones suggests that electrostatic effects play a minor role in these HO₂[•] reactions.

In general, the magnitude of $k_{\text{rxn}-2}$, which is in the order of $1-10^3 \text{ M}^{-1} \text{ s}^{-1}$, agrees well with the bimolecular rate constants observed experimentally in acidic solutions for the spin trapping of O₂^{•-} by nitrones.^{20,42} However, a plausible explanation for the difference in nucleophilicity between HO₂[•] and O₂^{•-} is that, although both are π -type radicals, their spin and charge density distributions are not very similar. For example, the spin density distribution and charge density on the attacking atom are 73% and -0.15 e for HO₂[•] and 50% and -0.50 e for O₂^{•-}, respectively. On the basis of the lower negative charge density and higher electron density distribution on the terminal O in HO₂[•] compared to O₂^{•-}, the nature of HO₂[•] radical addition to C=N of the nitrones can be predicted to be mostly electrophilic in nature rather than nucleophilic. Also, the presence of a low-lying first electronic excited-state in HO₂[•] can play a major role in determining the rate of its addition to nitrones, as observed in HO₂[•] reactions with some olefins.⁴³

To further evaluate if a charge-transfer mechanism was playing a role in determining the rate of HO₂[•] addition to nitrones, the electron affinities (EA) and ionization potentials (IP) for the nitrones were calculated at the PCM/mPW1K/6-31+G(d,p)//mPW1K/6-31+G(d,p) and PCM/B3LYP/6-31+G(d,p)//B3LYP/6-31G(d) levels (Table 4). However, results show that there is no correlation between the calculated $\Delta G_{\text{rxn}-2}$ or $k_{\text{rxn}-2}$ with the theoretical EA and IP values of these nitrones (see Figures S5–S8, Supporting Information). The same lack of correlation was observed using gas-phase energies at both levels of theory. The poor correlation between the rate constants and thermodynamic values could be due to the presence of H-bonding in the transition states that can bias the energies of the TS structures and this is further discussed below.

Unlike in the O₂^{•-} addition reactions,²⁵ a rationale for the trends observed for HO₂[•] addition favorability to some nitrones cannot be established based on calculated energies, rate constants, or electron-transfer mechanisms versus the charge density on C₂. However, there is a direct relationship between the kinetic parameters and strong H-bond interactions between the hydroperoxyl-H and the carbonyl-O in the TS structures that improve adduct formation, although the C₂–O₂H distances in all the TS structures are almost the same ($\sim 2.1 \text{ \AA}$). For example, at the mPW1K/6-31+G(d,p) level, EMAPO, DEPO, TAMPO, and CPCOMPO have strong interactions yielding a OOH---O=C distance from 1.76 to 1.87 \AA . The other adducts have OOH---NR₂ and OOH---O–N distances in the range of 2.07–2.42 \AA . The high $k_{\text{rxn}-2}$ value observed for EMPO cannot be rationalized in terms of strong H-bonding in the TS because the OOH---O–N distance observed was only 2.27 \AA , while CPCOMPO has stronger interactions yielding a OOH---O=C distance of 1.83 \AA but only gave a relatively small $k_{\text{rxn}-2}$ value of $61.9 \text{ M}^{-1} \text{ s}^{-1}$. Considering that the charge densities for CPCOMPO and EMPO are quite similar ($\sim 0.04 \text{ e}$), the difference in their reactivity could not be explained in terms of charge density on the C₂, electron affinity, or the presence of H-bonding in the TS.

IV. Conclusions

The reactivity of HO₂[•] toward various nitrones has been assessed from theoretical free energies of reaction, bimolecular rate constants, spin and charge densities, and hydrogen-bonding

interactions. The calculated rate constants are on the same order of magnitude as those observed experimentally for spin trapping in acidic aqueous solutions (i.e., $\sim 10^2-10^3 \text{ M}^{-1} \text{ s}^{-1}$). The transition state structures for HO₂[•] addition to the various nitrones are relatively early on the potential energy surface, as evidenced by the minor distortion of the bond angles around the nitronyl-C in the transition states. However, theoretically derived kinetic and thermodynamic parameters provide poor correlations with the calculated charge densities on the nitronyl-C (C₂, the site of radical addition), contrary to that observed for the reactivity of O₂^{•-} to nitrones,²⁵ an indication that the HO₂[•] addition to nitrones is not nucleophilic in nature. Strong H-bonding interactions between the hydroperoxyl-H and the carbonyl-O in the TS for some reactions play a significant role in facilitating HO₂[•] addition to nitrones. This observation suggests a need for strong H-bond acceptors in the design of nitrone-based antioxidants and spin traps for efficient HO₂[•] scavenging in biological systems.

Acknowledgment. This work is supported by NIH grant HL081248. J.L.Z. acknowledges support from the NIH grants HL38324, HL63744, and HL65608. C.M.H. acknowledges support from the NSF-funded Environmental Molecular Science Institute (CHE-0089147). The Ohio Supercomputer Center (OSC) is acknowledged for generous computational support of this research.

Supporting Information Available: Energies, enthalpies, and free energies for all spin traps and their corresponding spin adducts are available. This material is available free of charge at <http://pubs.acs.org>.

References and Notes

- Halliwell, B. *Oxidative Stress and Disease* **2001**, *7*, 1–16; Halliwell, B. *Drugs Aging* **2001**, *18*, 685–716; Zweier, J. L.; Talukder, M. A. H. *Cardiovasc. Res.* **2006**, *70*, 181–190; Zweier, J. L.; Villamena, F. A. In *Oxidative Stress and Cardiac Failure*; Kukin, M. L., Fuster, V., Eds.; Futura Publishing: Armonk, NY, 2003, pp 67–95.
- Sawyer, D. T.; Chiericato, G., Jr.; Angelis, C. T.; Nanni, E. J., Jr.; Tsuchiya, T. *Anal. Chem.* **1982**, *54*, 1720–1724.
- Behar, D.; Czapski, G.; Rabani, J.; Dorfman, L. M.; Schwarz, H. A. *J. Phys. Chem.* **1970**, *74*, 3209–3213.
- Czapski, G.; Bielski, B. H. J. *J. Phys. Chem.* **1963**, *67*, 2180–2184.
- Halliwell, B.; Gutteridge, J. M. C. *Free Radicals in Biology and Medicine*; Oxford University Press: New York, 1999.
- Cheng, Z.; Li, Y. *Chem. Rev.* **2007**, *107*, 748–766.
- Zweier, J. L.; Broderick, R.; Kuppusamy, P.; Thompson-Gorman, S.; Luty, G. A. *J. Biol. Chem.* **1994**, *269*, 24156–24162.
- Zweier, J. L.; Flaherty, J. T.; Weisfeldt, M. L. *Proc. Natl. Acad. Sci. U.S.A.* **1987**, *84*, 1404; Zweier, J. L.; Kuppusamy, P.; Luty, G. A. *Proc. Natl. Acad. Sci. U.S.A.* **1988**, *85*, 4046; Zweier, J. L.; Kuppusamy, P.; Williams, R.; Rayburn, B. K.; Smith, D.; Weisfeldt, M. L.; Flaherty, J. T. *J. Biol. Chem.* **1989**, *264*, 18890.
- Ambrosio, G.; Zweier, J. L.; Flaherty, J. T. *J. Mol. Cell Cardiol.* **1991**, *23*, 1359–1374.
- Janzen, E. G. *Free Radical Biol. Med.* **1980**, *4*, 115–154; Janzen, E. G. *Acc. Chem. Res.* **1971**, *4*, 31–40; Janzen, E. G.; Haire, D. L. *Adv. Free Radical Chem.* **1990**, *1*, 253–295; *Toxicology of the Human Environment. The Critical Role of Free Radicals*; Rhodes, C. J., Ed.; Taylor and Francis: London, 2000; Rosen, G. M.; Britigan, B. E.; Halpern, H. J.; Pou, S. *Free Radicals: Biology and Detection by Spin Trapping*; Oxford University Press: New York, 1999; Villamena, F. A.; Zweier, J. L. *Antioxid. Redox Signaling* **2004**, *6*, 619–629.
- Villamena, F. A.; Merle, J. K.; Hadad, C. M.; Zweier, J. L. *J. Phys. Chem. A* **2005**, *109*, 6083–6088.
- Nonogawa, M.; Arai, T.; Endo, N.; Pack, S. P.; Kodaki, T.; Makino, K. *Org. Biomol. Chem.* **2006**, *4*, 1811–1816; Zhang, H.; Joseph, J.; Vasquez-Vivar, J.; Karoui, H.; Nsanzumuhire, C.; Martasek, P.; Tordo, P.; Kalyanaraman, B. *FEBS Lett.* **2000**, *473*, 58–62.
- Breuer, E.; Aurich, H. G.; Nielsen, A. *Nitrones, Nitronates and Nitroxides*; John Wiley and Sons: New York, 1989.

- (14) Floyd, R. A. *Aging Cell* **2006**, *5*, 51–57; Nakae, D.; Kishida, H.; Enami, T.; Konishi, Y.; Hensley, K. L.; Floyd, R. A.; Kotake, Y. *Cancer Sci.* **2003**, *94*, 26–31; Nakae, D.; Uematsu, F.; Kishida, H.; Kusuoka, O.; Katsuda, S.-i.; Yoshida, M.; Takahashi, M.; Maekawa, A.; Denda, A.; Konishi, Y.; Kotake, Y.; Floyd, R. A. *Cancer Lett. (Amsterdam, Netherlands)* **2004**, *206*, 1–13; Becker, D. A.; Ley, J. J.; Echevoyen, L.; Alvarado, R. *J. Am. Chem. Soc.* **2002**, *124*, 4678; Ginsberg, M. D.; Becker, D. A.; Busto, R.; Belayev, A.; Zhang, Y.; Khoutorova, L.; Ley, J. J.; Zhao, W.; Belayev, L. *Ann. Neurol.* **2003**, *54*, 330.
- (15) Floyd, R. A.; Hensley, K. *Ann. New York Acad. Sci.* **2000**, 899, 222–237.
- (16) *Handbook of Synthetic Antioxidants*; Packer, L., Cadenas, E., Eds.; Marcel Dekker, Inc.: New York, 1997.
- (17) Fong, J. J.; Rhoney, D. H. *Ann. Pharmacother.* **2006**, *40*, 461–471; Maples, K. R.; Green, A. R.; Floyd, R. A. *CNS Drugs* **2004**, *18*, 1071–1084; Zhao, Z.; Cheng, M.; Maples, K. R.; Ma, J. Y.; Buchan, A. M. *Brain Res.* **2001**, *909*, 46–50.
- (18) Konorev, E. A.; Baker, J. E.; Joseph, J.; Kalyanaraman, B. *Free Radical Biol. Med.* **1993**, *14*, 127–37; Pietri, S.; Liebgott, T.; Frijaville, C.; Tordo, P.; Culcasi, M. *Eur. J. Biochem.* **1998**, *254*, 256–265.
- (19) Lapchak, P. A.; Araujo, D. M.; Song, D.; Wei, J.; Purdy, R.; Zivin, J. A. *Stroke* **2002**, *33*, 1665–1670; Tosaki, A.; Blasig, I. E.; Pali, T.; Ebert, B. *Free Radical Biol. Med.* **1990**, *8*, 363–72.
- (20) Finkelstein, E.; Rosen, G. M.; Rauckman, E. J. *J. Am. Chem. Soc.* **1980**, *102*, 4995.
- (21) Boyd, S. L.; Boyd, R. J. *J. Phys. Chem.* **1994**, *98*, 11705–11713.
- (22) Villamena, F. A.; Hadad, C. M.; Zweier, J. L. *J. Phys. Chem. A* **2005**, *109*, 1662–1674.
- (23) Bosnjakovic, A.; Schlick, S. *J. Phys. Chem. B* **2006**, *110*, 10720–10728; Panchenko, A.; Dilger, H.; Kerres, J.; Hein, M.; Ullrich, A.; Kaz, T.; Roduner, E. *Phys. Chem. Chem. Phys.* **2004**, *6*, 2891–2894; Yang, J.; Chen, C.; Ji, H.; Ma, W.; Zhao, J. *J. Phys. Chem. B* **2005**, *109*, 21900–21907; Yu, J.; Chen, J.; Li, C.; Wang, X.; Zhang, B.; Ding, H. *J. Phys. Chem. B* **2004**, *108*, 2781–2783; Vakrat-Haglilili, Y.; Weiner, L.; Brumfeld, V.; Brandis, A.; Salomon, Y.; McLlroy, B.; Wilson, B. C.; Pawlak, A.; Rozanowska, M.; Sarna, T.; Scherz, A. *J. Am. Chem. Soc.* **2005**, *127*, 6487–6497; Nam, S.-N.; Han, S.-K.; Kang, J. W.; Choi, H. *Ultrason. Sonochem.* **2003**, *10*, 39–147; Balakirev, M. Y.; Khramtsov, V. V. *J. Org. Chem.* **1996**, *61*, 7263–7269.
- (24) Chen, Y.-R.; Chen, C.-L.; Yeh, A.; Liu, X.; Zweier, J. L. *J. Biol. Chem.* **2006**, *281*, 13159–13168; Dugan, L. L.; Sensi, S. L.; Canzoniero, L. M. T.; Handran, S. D.; Rothman, S. M.; Lin, T. S.; Goldberg, M. P.; Choi, D. W. *J. Neurosci.* **1995**, *15*, 6377–6388; Partridge, R. S.; Monroe, S. M.; Parks, J. K.; Johnson, K.; Parker, W. D., Jr.; Eaton, G. R.; Eaton, S. S. *Arch. Biochem. Biophys.* **1994**, *310*, 210–217; Nohl, H.; Jordan, W.; Hegner, D. *FEBS Lett.* **1981**, *123*, 241–244; Wang, P.; Chen, H.; Qin, H.; Sankarapandi, S.; Becher, M. W.; Wong, P. C.; Zweier, J. L. *Proc. Natl. Acad. Sci. U.S.A.* **1998**, *95*, 4556–4560.
- (25) Villamena, F. A.; Xia, S.; Merle, J. K.; Lauricella, R.; Tuccio, B.; Hadad, C. M.; Zweier, J. L. *J. Am. Chem. Soc.* **2007**, *129*, 8177–8191.
- (26) Frisch, M. J.; Trucks, G. W.; Schlegel, H. B.; Scuseria, G. E.; Robb, M. A.; Cheeseman, J. R.; Montgomery, J. A., Jr.; Vreven, T.; Kudin, K. N.; Burant, J. C.; Millam, J. M.; Iyengar, S. S.; Tomasi, J.; Barone, V.; Mennucci, B.; Cossi, M.; Scalmani, G.; Rega, N.; Petersson, G. A.; Nakatsuji, H.; Hada, M.; Ehara, M.; Toyota, K.; Fukuda, R.; Hasegawa, J.; Ishida, M.; Nakajima, T.; Honda, Y.; Kitao, O.; Nakai, H.; Klene, M.; Li, X.; Knox, J. E.; Hratchian, H. P.; Cross, J. B.; Bakken, V.; Adamo, C.; Jaramillo, J.; Gomperts, R.; Stratmann, R. E.; Yazyev, O.; Austin, A. J.; Cammi, R.; Pomelli, C.; Ochterski, J. W.; Ayala, P. Y.; Morokuma, K.; Voth, G. A.; Salvador, P.; Dannenberg, J. J.; Zakrzewski, V. G.; Dapprich, S.; Daniels, A. D.; Strain, M. C.; Farkas, O.; Malick, D. K.; Rabuck, A. D.; Raghavachari, K.; Foresman, J. B.; Ortiz, J. V.; Cui, Q.; Baboul, A. G.; Clifford, S.; Cioslowski, J.; Stefanov, B. B.; Liu, G.; Liashenko, A.; Piskorz, P.; Komaromi, I.; Martin, R. L.; Fox, D. J.; Keith, T.; Al-Laham, M. A.; Peng, C. Y.; Nanayakkara, A.; Challacombe, M.; Gill, P. M. W.; Johnson, B.; Chen, W.; Wong, M. W.; Gonzalez, C.; Pople, J. A. *Gaussian 03*, revision B.05; Gaussian, Inc.: Wallingford, CT, 2004.
- (27) Labanowski, J. W.; Andzelm, J. *Density Functional Methods in Chemistry*; Springer: New York, 1991; Parr, R. G.; Yang, W. *Density Functional Theory in Atoms and Molecules*; Oxford University Press: New York, 1989.
- (28) Becke, A. D. *Phys. Rev.* **1988**, *38*, 3098–3100; Lee, C.; Yang, W.; Parr, R. G. *Phys. Rev. B* **1988**, *37*, 785–789; Becke, A. D. *J. Chem. Phys.* **1993**, *98*, 1372–1377; Hehre, W. J.; Radom, L.; Schleyer, P. V.; Pople, J. A. *Ab Initio Molecular Orbital Theory*; John Wiley & Sons: New York, 1986.
- (29) Lynch, B. J.; Fast, P. L.; Harris, M.; Truhlar, D. G. *J. Phys. Chem. A* **2000**, *104*, 4811.
- (30) Tomasi, J.; Persico, M. *Chem. Rev.* **1994**, *94*, 2027–2094; Cossi, M.; Barone, V.; Cammi, R.; Tomasi, J. *Chem. Phys. Lett.* **1996**, *255*, 327–335; Barone, V.; Cossi, M.; Tomasi, J. *J. Chem. Phys.* **1997**, *107*, 3210; Barone, V.; Cossi, M.; Tomasi, J. *J. Comput. Chem.* **1998**, *19*, 404; Cossi, M.; Barone, V. *J. Chem. Phys.* **1998**, *109*, 6246.
- (31) Scott, A. P.; Radom, L. *J. Phys. Chem.* **1996**, *100*, 16502–16513.
- (32) Lynch, B. J.; Truhlar, D. G. *J. Phys. Chem. A* **2001**, *105*, 2936.
- (33) Reed, A. E.; Curtiss, L. A.; Weinhold, F. A. *Chem. Rev.* **1988**, *88*, 899–926.
- (34) Barckholtz, C.; Barckholtz, T. A.; Hadad, C. M. *J. Phys. Chem. A* **2001**, *105*, 140–152.
- (35) Laidler, K. J. *Chemical Kinetics*; Harper & Row: New York, 1987.
- (36) Wigner, E. P. *Z. Phys. Chem. Abt. B* **1932**, *19*, 203.
- (37) Villamena, F.; Dickman, M. H.; Crist, D. R. *Inorg. Chem.* **1998**, *37*, 1446–1453; Boeyens, J. C. A.; Kruger, G. J. *Acta Crystallogr., Sect. B* **1970**, *26*, 668; Xu, Y. K.; Chen, Z. W.; Sun, J.; Liu, K.; Chen, W.; Shi, W.; Wang, H. M.; Zhang, X. K.; Liu, Y. J. *J. Org. Chem.* **2002**, *67*, 7624–7630.
- (38) Alini, S.; Citterio, A.; Farina, A.; Fochi, M. C.; Malpezzi, L. *Acta Crystallogr. Part C* **1998**, *54*, 1000–1003.
- (39) DeMatteo, M. P.; Poole, J. S.; Shi, X.; Sachdeva, R.; Hatcher, P. G.; Hadad, C. M.; Platz, M. S. *J. Am. Chem. Soc.* **2005**, *127*, 7094–7109.
- (40) Villamena, F. A.; Rockenbauer, A.; Gallucci, J.; Velayutham, M.; Hadad, C. M.; Zweier, J. L. *J. Org. Chem.* **2004**, *69*, 7994–8004.
- (41) Buettner, G. R. *Arch. Biochem. Biophys.* **1993**, *300*, 535–543.
- (42) Tsai, P.; Ichikawa, K.; Mailer, C.; Pou, S.; Halpern, H. J.; Robinson, B. H.; Nielsen, R.; Rosen, G. M. *J. Org. Chem.* **2003**, *68*, 7811–7817.
- (43) Stark, M. S. *J. Am. Chem. Soc.* **2000**, *122*, 4162–4170; Stark, M. S. *J. Phys. Chem. A* **1997**, *101*, 8296–8301.
- (44) Clifford, E. P.; Wenthold, P. G. G., R.; Lineberger, W. C.; DePuy, C. H.; Bierbaum, V. M.; Ellison, G. B. *J. Chem. Phys.* **1998**, *109*, 10293.